

Received: 2015.07.16  
Accepted: 2015.08.30  
Published: 2015.XX.XX

# Diminished Resistance to Hyperoxia in Brains of Reproductively Senescent Female CBA/H Mice

## Authors' Contribution:

Study Design A  
Data Collection B  
Statistical Analysis C  
Data Interpretation D  
Manuscript Preparation E  
Literature Search F  
Funds Collection G

ABCDEF 1 **Ana Šarić\***  
ACDE 1 **Sandra Sobočanec\***  
BCE 1 **Željka Mačak Šafranko**  
BCD 1 **Marijana Popović Hadžija**  
BCD 2 **Robert Bagarić**  
BCD 2 **Vladimir Farkaš**  
AG 2 **Alfred Švarc**  
AG 1 **Tatjana Marotti**  
EFG 1 **Tihomir Balog**

1 Division of Molecular Medicine, Ruđer Bošković Institute, Zagreb, Croatia,  
2 Division of Experimental Physics, Ruđer Bošković Institute, Zagreb, Croatia

\* Ana Šarić and Sandra Sobočanec contributed equally to this work

## Corresponding Author:

Sandra Sobočanec, e-mail: [ssoboc@irb.hr](mailto:ssoboc@irb.hr)

## Source of support:

The research is funded by Croatian Ministry of Science, Education and Sports, Grant No. 098-0982464-1647 and No. 098-0982464-2460. FP7-REGPOT-2012-2013-1, Grant Agreement Number 316289 – InnoMol

## Background:

We have explored sex differences in ability to maintain redox balance during acute oxidative stress in brains of mice. We aimed to determine if there were differences in oxidative/antioxidative status upon hyperoxia in brains of reproductively senescent CBA/H mice in order to elucidate some of the possible mechanisms of lifespan regulation.

## Material/Methods:

The brains of 12-month-old male and female CBA/H mice (n=9 per sex and treatment) subjected to 18-h hyperoxia were evaluated for lipid peroxidation (LPO), antioxidative enzyme expression and activity - superoxide dismutase 1 and 2 (Sod-1, Sod-2), catalase (Cat), glutathione peroxidase 1 (Gpx-1), heme-oxygenase 1 (Ho-1), nad NF-E2-related factor 2 (Nrf2), and for 2-deoxy-2-[<sup>18</sup>F] fluoro-D-glucose (<sup>18</sup>FDG) uptake.

## Results:

No increase in LPO was observed after hyperoxia, regardless of sex. Expression of Nrf-2 showed significant downregulation in hyperoxia-treated males (p=0.001), and upregulation in hyperoxia-treated females (p=0.023). Also, in females hyperoxia upregulated Sod-1 (p=0.046), and Ho-1 (p=0.014) genes. SOD1 protein was upregulated in both sexes after hyperoxia (p=0.009 for males and p=0.011 for females). SOD2 protein was upregulated only in females (p=0.008) while CAT (p=0.026) and HO-1 (p=0.042) proteins were increased after hyperoxia only in males. Uptake of <sup>18</sup>FDG was decreased after hyperoxia in the back brain of females.

## Conclusions:

We found that females at their reproductive senescence are more susceptible to hyperoxia, compared to males. We propose this model of hyperoxia as a useful tool to assess sex differences in adaptive response to acute stress conditions, which may be partially responsible for observed sex differences in longevity of CBA/H mice.

## MeSH Keywords:

**Cell Aging • Fluorodeoxyglucose F18 • Hyperoxia • Mice, Inbred CBA • Neuroimaging**

## Full-text PDF:

<http://www.basic.medscimonit.com/abstract/index/idArt/895356>

 3490

 2

 5

 42



## 1 Background

The most popular hypothesis used to explain the mechanism of ageing is the Free Radical Theory of Aging (reviewed in [1,2], originally proposed by Denham Harman more than 50 years ago [3]. This theory holds that accumulation of reactive oxygen species (ROS)-induced oxidative damage of macromolecules underlies the ageing process. ROS are produced as a result of normal cellular metabolism, mainly in mitochondria and peroxisomes, as well as from many cytosolic enzyme systems [2]. Postmitotic cells such as neurons suffer more oxidative damage and are more affected by ageing than are mitotic cells [4]. Numerous studies highlight the role of ROS in neuronal cell death and neurodegeneration [5]. Since sexual selection can also influence lifespan and survival rates [6], an alternative approach to study ageing and longevity is to investigate sex differences in response to oxidative stress during aging. In most mammals, including humans, life expectancy is female-biased [6]. Hyperoxia is considered as one of the oldest oxidative stressors used to assess defence response to oxidative stress [1]. In *Drosophila melanogaster*, hyperoxia reduces lifespan [1], induces the same level of oxidative damage [7] and similar gene expression patterns as ageing [8]. Thus, normobaric hyperoxia may serve as a good model for studying ageing process because both hyperoxia and aging share some common links. The 3 major antioxidant enzymes that eliminate excess ROS and define the potential to cope with the oxidative stress are superoxide dismutase (SOD), catalase (CAT), and glutathione peroxidase (GPx). Heme oxygenase (HO) is the rate-limiting enzyme for heme degradation in mammals. It is a stress-response enzyme, highly induced by a variety of agents causing oxidative stress, hypoxia, hyperoxia, and proinflammatory cytokines [8], and as such is regarded as a sensitive and reliable indicator of cellular oxidative stress. In response to oxidative stress, HO-1 induction provides cell protection by promoting the catabolism of pro-oxidant metalloporphyrins to bile pigments (biliverdin and bilirubin) which are considered to have free radical scavenging properties [9]. Nrf2 is a transcription factor that plays a key role in the transcriptional induction of phase II detoxification enzymes and endogenous antioxidants. Accumulating evidence has been provided indicating protective role of Nrf2 against many pathological conditions, including age-related diseases and aging [9]. Moreover, we have measured brain glucose uptake using positron emission tomography (PET), as a marker of brain bioenergetic capacity. The uptake and distribution of radioactive glucose analogue  $^{18}\text{F}$ FDG is a qualitative and quantitative indicator of tissue functionality and damage. The  $^{18}\text{F}$ FDG PET technology is found to be potentially very useful tool for the assessment of the efficacy of antitumor therapy [10]. The negative correlation of glucose consumption and oxidative stress in the brain was described in recent papers [11]. Also, the association between glucose consumption and different types of stress was

documented in several studies [12,13]. In this study, we explored sex differences in oxidative/antioxidative status in brain of CBA/H mice that entered reproductive senescence and their ability to maintain redox balance upon acute oxidative stress load. For this purpose, we employed normobaric hyperoxia as a model of oxidative stress. LPO, Sod-1, Sod-2, Cat, Gpx-1, Ho-1 and NF-E2-related factor 2 (Nrf-2) were determined as a measure of oxidative/antioxidative status. Studies using female animals have shown that 17- $\beta$ -estradiol ( $\text{E}_2$ ) can act as a mediator of higher glucose consumption [14, 15]. In our previous studies we showed female-biased resistance to oxidative stress in young adult mice [16] that was in relationship with protective effect of  $\text{E}_2$  [17]. Since most metabolic studies have been conducted in only one sex, little attention has been paid to understanding the sex specificity of the above mentioned molecular pathways [18]. In this regard, we investigated potential gender difference in brain oxidative/antioxidative status and glucose metabolism of reproductively senescent animals in response to acute oxidative stress load.

## Material and Methods

### Animals and experimental design

The experiments were performed in accordance with the current laws of the Republic of Croatia and with the guidelines of European Community Council Directive of November 24, 1986 (86/609/EEC). All applicable institutional and/or national guidelines for the care and use of animals were followed. Twelve months old male and female CBA/H mice from breeding colony of the Ruđer Bošković Institute (Zagreb, Croatia) were maintained under the following laboratory conditions: 12-h light/day cycle,  $22\pm 2^\circ\text{C}$  room temperature; access to food pellets and tap water ad libitum. In this study total of 36 animals were used. Schematic diagram of the experimental groups is presented in Figure 1. Hyperoxic oxygen conditions were carried out by flushing the chamber (Đuro Đaković, Slavonski Brod, Croatia) with pure oxygen (25 L/min for 10 minutes) to replace air. Normoxic  $\text{O}_2$  conditions serving as a control were obtained by keeping mice in the same chamber, but under ambient air. The animals were divided into two groups: control ( $n=9$ ), receiving normoxic oxygen (21%  $\text{O}_2$ ) and hyperoxia-treated ( $n=9$ ), receiving pure oxygen (95%  $\text{O}_2$ ) for 18 hours. Two animals from each group were randomly chosen and recorded for the PET scan analysis. After the analysis, animals were euthanized by cervical dislocation. The brains from animals used in PET scan analysis were not used for other experiments. For biochemical analyses, each group consisted of seven animals. Briefly, after exposure to normoxic air/pure oxygen, mice were euthanized by cervical dislocation and brains were immediately rinsed in cold 50mM PBS ( $\text{pH}=7.8$ ) and subjected to further analyses.

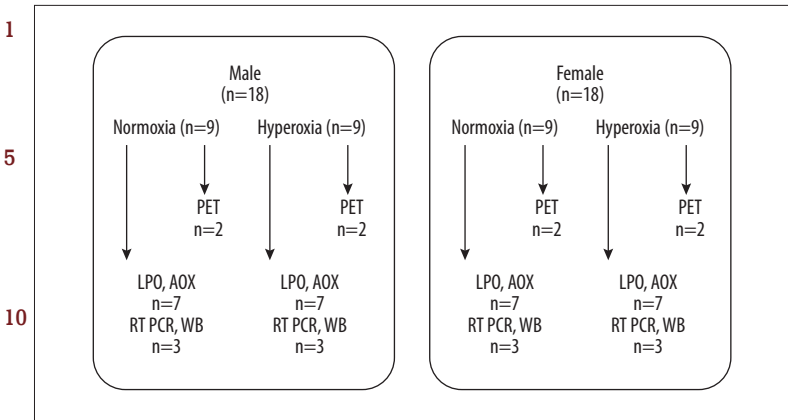


**Figure 1.** Schematic diagram of the experimental groups used in this study. LPO-lipid peroxidation; AOX-antioxidative enzyme activities; RT-PCR: real-time PCR; WB-western blot.

**Table 1.** Primers used for quantitative real-time PCR analysis.

Gene	Assay ID	Product size (bp)
<i>Sod-1</i>	Mm01344233_g1	71
<i>Sod-2</i>	Mm01313000_m1	67
<i>Cat</i>	Mm00437992_m1	64
<i>Gpx-1</i>	Mm00656767_g1	134
<i>Ho-1</i>	Mm00516007_m1	92
<i>Nrf-2</i>	Mm00772789_m1	65
<i>Gapdh</i>	Mm99999915_g1	107

**Preparation of cytosolic, mitochondrial and microsomal fractions**

In all groups the brains were first separated into left and right hemisphere using stereo microscope SteREO Discovery.V8 (Carl Zeiss, Gottingen, Germany). Right hemisphere was used for RNA isolation, while left hemisphere was subjected to cellular fractionation. Briefly, fresh brains were immediately homogenized with TRIS-HCl (10mM) and sucrose (0.25M, pH=7.4) at 4°C (20% w/v). Cytosolic fraction was prepared as described by [19]. Microsomal fractions were prepared as described by [20], while mitochondrial fractions were prepared as described by [21]. Microsomal pellet was resuspended in 50 mM TRIS-HCl and 0.15 M KCl (pH=7.4), quickly frozen in liquid nitrogen, and stored at -80°C. Mitochondrial pellet was resuspended in isolation buffer (250 mM sucrose, 2mM EGTA, 0.5% fatty acid free BSA, 20 mM Tris-HCl, pH=7.4). All fractions were stored at -80°C until further analyses.

**Lipid peroxidation assay**

The lipid oxidative damage was carried out on brain microsomes using LPO assay kit (Bioxytech® LPO-586™, OXIS International, Inc. Foster City, CY, USA) according to the manufacturer protocol. In this study the malondialdehyde (MDA) alone was measured [22].

**Assay for antioxidative enzyme activities**

All enzyme activities were assayed spectrophotometrically using Camspec M330 spectrophotometer equipped with M330 Camspec software package (Camspec LTD. Cambridge, UK). Gpx-1 [23], Cat [24] and Sod-1 [25] were assayed in cytosolic fraction. Sod-2 activity was determined in mitochondrial fraction [25].

**RNA isolation and quantitative real-time PCR analysis.**

Total RNA was extracted using TRIzol reagent (Invitrogen, Carlsbad, CA, USA) according to the manufacturer's instructions. Reverse transcription and real-time PCR analysis were done as described previously [16], to quantify relative mRNA expression of Sod1, Sod2, Cat, Gpx-1, Ho-1 and Nrf-2. Using the 2<sup>-ΔΔCt</sup> method, data are presented as the fold-change in Sod1, Sod2, Cat, Gpx-1, Ho-1 and Nrf-2 gene expression normalized to endogenous reference gene (β-actin) and relative to the untreated control. Assays used in this study are listed in Table 1. All reactions were carried out in triplicate.

**Western blot analysis**

Eighty micrograms of total proteins from pool of three samples per each experimental group were subjected to 10% or 12.5%

1 SDS-PAGE according to the method previously described [26]. Western blotting was performed using the primary polyclonal rabbit anti-mouse Sod1, Sod2, Cat, Gpx-1, Ho-1 or Nrf-2 antibody (Abcam, Cambridge, UK), following donkey anti-rabbit  
5 IgG horseradish peroxidase-conjugated secondary antibody (Amersham Biosciences Inc., USA). Anti-ERK-2 (C-14, Santa Cruz Biotechnology, Inc., USA) was used as a loading control. After the immunodetection the chemiluminescence signals were detected with the Alliance 4.7 Imaging System (UVITEC, Cambridge, UK).

10

### Determination of protein concentration

Protein concentration in supernatant was estimated by the method as described in previous report [27] using bovine serum albumin as a standard.

15

### <sup>18</sup>FDG-microPET imaging

For <sup>18</sup>FDG-microPET imaging, animals have been anesthetized  
20 in induction chamber with 4% isoflurane (Forane, Abbott laboratories, UK) in 100% oxygen with delivery rate of 0.6 l/min and intraperitoneally injected with 100–200 µl of solution containing 45 MBq of radiotracer [<sup>18</sup>F] Fluoro-2-deoxy-2-D-glucose (<sup>18</sup>FDG). To avoid the influence of warming on <sup>18</sup>FDG biodistribution in mice injected intra venous, in our experiments  
25 we used intraperitoneally model of <sup>18</sup>FDG administration described by [28]. Using this experimental model we have provided the biodistribution of <sup>18</sup>FDG in mice brain after 1 hour is same as is in first minutes after intra venous application of  
30 <sup>18</sup>FDG. At 1 hour postinjection of <sup>18</sup>FDG, each animal has been put into the ClearPet camera (Raytest with resolution of 1.2 mm in the central FOV) and kept warm at the comfortable temperature of 36.5°C during the whole procedure. During scanning anaesthesia was maintained with 2% isoflurane in 100%  
35 oxygen with delivery rate of 0.6 l/min. We performed 22 consecutive 2 minutes measurements to eliminate the possibility of in-measurement shift of animal position, and when the immobility of the animal throughout of experiment was established, we have summarized the data in the whole period  
40 of measurement, and got results equivalent to 44 minutes of continuous monitoring. The final result is given in standardized uptake value units (SUV) which is defined as:

45

$$SUV = \frac{\text{MeasuredActivity} \left[ \frac{MBq}{ml} \right]}{\text{TotalActivity} \left[ \frac{MBq}{body\ weight\ [g]} \right]}$$

### <sup>18</sup>FDG brain uptake data analysis

Image reconstruction was done using OSMAPSL iterative reconstruction algorithm incorporated in commercial ClearPET image reconstruction software. Data analysis was performed using PMOD 3.2 image analysis software normalized and calibrated prior to experiment with known activity. We have first

analyzed and compared all 22 time frames to confirm the immobility of the animal. In this study there were no observed movements of animals. Then we summarized and averaged all time frames to obtain the static data image equivalent to 44 minutes of continuous data acquisition. We have performed our data analysis in two-step procedure. First we have looked for qualitative features establishing the qualitative effects using PMOD 3D imaging software (PMOD Technologies Ltd., Zurich, Switzerland) and then we have quantified it using PMOD 2D analysis, and accompanying numerical software packages.

1

5

10

### PET image of brain co-registered with mouse brain atlas

Co-registration was made in PMOD FUSION software mode. In the first step PET image of mouse brain was co-registered  
15 with mouse head CT template from PMOD software. Mouse brain MRI template is another template available in PMOD software which is co-registered with head CT template by default. That means if PET image is co-registered with head CT template in first step, it is also co-registered with brain MRI  
20 template. In the second step [29,30] is used for the analysis of mouse brain PET data. Brain atlas is also available in PMOD and it divides brain MRI template into 19 volumes of interest (brain regions). Of these 19 regions, 8 were selected (cerebellum, brainstem, central grey, left and right mid brain, left  
25 and right inferior and superior colliculi) as brain regions of interest and were merged in 1 volume of interest named “back brain”. The same brain regions were used for determination and calculate percentage of <sup>18</sup>FDG uptake in back brain of tested animals in all images of normoxia- and hyperoxia-treated  
30 mice. Percentage of back brain uptake in the whole brain uptake was calculated by putting in ratio <sup>18</sup>FDG uptake in 8 back brain regions with <sup>18</sup>FDG uptake in all 19 region of brain atlas.

### Statistical analysis

35

Statistical analysis of the data was performed using R v2.15.3 (CRAN, <http://cran.r-project.org>) and Studio for Windows, v0.97 (<http://www.rstudio.com/>) for all experiments, except for the real-time PCR analysis, where relative gene expression of each gene  
40 was calculated using the Relative Expression Software Tool (REST) by the method of [31]. All groups were tested for normality of distribution using Shapiro-Wilk test. Since data followed normal distribution, the differences between two groups were tested using Student's t-test. Statistical significance was set at p<0.05.

45

## Results

### The effect of hyperoxia on lipid peroxidation

50

As a measure of lipid oxidative stress, we have determined the MDA levels in brain of hyperoxia-treated CBA/H mice (Table 2).

53

**Table 2.** Oxidative damage (lipid peroxidation – MDA production) and antioxidative parameters (antioxidant enzyme activity) in brain supernatant 12 months old control (C) and hyperoxia-treated (H) CBA mice of both sexes. Data are mean ±SEM and are analyzed by Student's t-test.

Parameter	Males		Females	
	Normoxia	Hyperoxia	Normoxia	Hyperoxia
MDA (nmol/mg proteins)	2.72±0.25	2.63±0.12	2.33±0.17	2.71±0.13
Sod-1 (IU/mg proteins)	0.56±0.05	0.59±0.06	0.45±0.02 <sup>#</sup>	0.53±0.03
Sod-2 (IU/mg proteins)	4.05±0.53	3.40±0.41	3.21±0.29	3.96±0.56
Cat (IU/mg proteins)	1.79±0.26	2.20±0.12	2.08±0.19	1.89±0.09
Gpx-1 (IU/mg proteins)	0.68±0.08	0.74±0.01	0.83±0.07	0.97±0.09 <sup>*</sup>

Sod-1 <sup>#</sup> p=0.040, normoxia females vs. normoxia males; Gpx-1 <sup>\*</sup> p=0.040, normoxia females vs. hyperoxia females

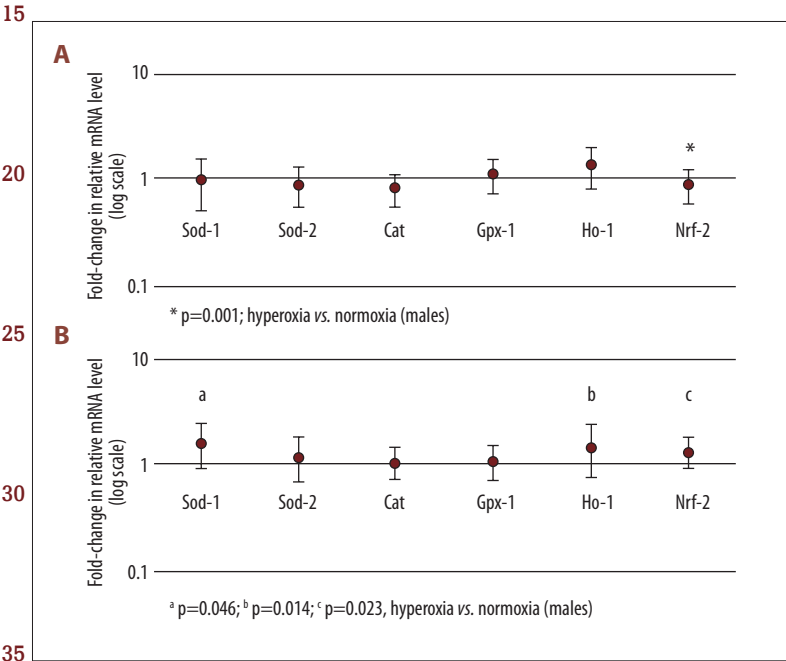


**Figure 2.** Real-time PCR analysis of Sod1, Sod2, Cat, Gpx-1, Ho-1 and Nrf-2 mRNA level in brain of control and hyperoxia-treated CBA/H male (A) and female (B) mice. Data are presented as mean relative fold-change ±S.E. compared to normoxia as control (defined as 1). For males, normoxia vs. hyperoxia: \* Nrf-2 (fold-change -1.101, p=0.001). For females normoxia vs. hyperoxia: <sup>a</sup> Sod-1 (fold-change 1.296, p=0.046); <sup>b</sup> Ho-1 (fold-change 1.232, p=0.014); <sup>c</sup> Nrf-2 (fold-change 1.167, p=0.023).

The level of MDA did not show statistically significant change after hyperoxia treatment in any sex examined.

**40 The effect of hyperoxia on antioxidative enzyme activity and expression**

In order to investigate antioxidative enzyme defences in response to hyperoxia, the enzymatic activities of Sod-1, Sod-2, Cat, and Gpx-1 were measured in brain of CBA/H mice of both sexes (Table 2). We found no change in activities upon treatment of neither Sod isoforms. The only change observed was the initial lower activity of Sod-1 in normoxia females compared to normoxia males (p=0.040). Considering Cat and Gpx-1 activities, while Cat activity remained unchanged irrespective of sex or treatment, slight increase in Gpx-1 activity was observed in hyperoxia-treated, compared to normoxia-treated females (p=0.04). These results suggest the absence of oxidative stress or adaptive response

upon oxidative insult. Real-time PCR analysis of relative Sod-1, Sod-2, Cat, Gpx-1, Ho-1 and Nrf-2 gene expression in the brain of mice subjected to hyperoxia is shown in Figure 2. In males only Nrf-2 showed slight, but significant downregulation in hyperoxia-treated group (fold-change -1.101, p=0.001), while none of the antioxidative genes changed their expression after hyperoxia treatment (Figure 2A). In females, hyperoxia significantly upregulated Sod-1 (fold-change 1.296, p=0.046), Ho-1 (fold-change 1.232, p=0.014), and Nrf-2 (fold-change 1.167, p=0.023). Sod-2, Cat and Gpx-1 gene expression remained unchanged in these samples (Figure 2B). Western blot analysis of Sod-1, Sod-2, Cat, Gpx-1, Ho-1 and Nrf-2 protein expression in the brain of mice subjected to hyperoxia is shown on Figure 3A for males and Figure 3B for females. The level of Sod-1 protein was upregulated in both sexes (<sup>a</sup> p=0.009 for males, \* p=0.011 for females) in hyperoxia treated samples, when compared to control. Contrary to Sod-1, Sod-2 protein was consistently upregulated in



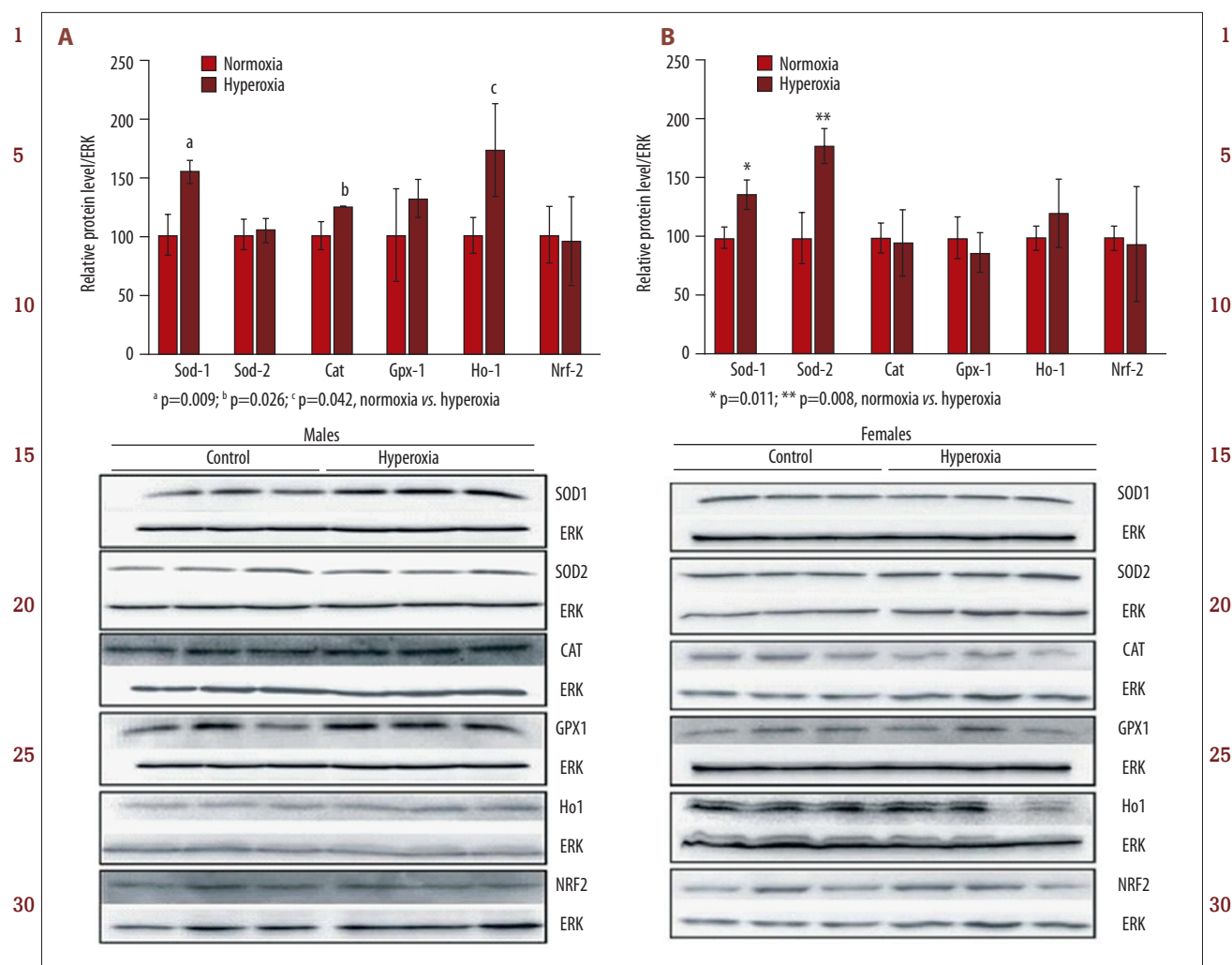


**Figure 3.** Representative western blots of Sod-1, Sod-2, Cat, Gpx-1, Ho-1 and Nrf-2 protein level in brain of normoxia- and hyperoxia-exposed CBA/H male (A) and female (B) mice (n=3 per group). Results are presented as mean±SEM of three mice per group. Protein intensities are expressed relative to ERK content. For males: <sup>a</sup> p=0.009; <sup>b</sup> p=0.026; <sup>c</sup> p=0.042, normoxia vs. hyperoxia. For females: <sup>\*</sup> p=0.011; <sup>\*\*</sup> p=0.008, normoxia vs. hyperoxia.

female brain after hyperoxia while at the same time remained unchanged in males (<sup>\*\*</sup> p=0.008). The expression of Cat protein was increased in hyperoxia-exposed males, compared to their corresponding control (<sup>b</sup> p=0.026), while in females there was no change in protein expression upon hyperoxia. The expression of Gpx-1 protein was unchanged after hyperoxia in both sexes. Hyperoxia significantly upregulated Ho-1 protein only in males after hyperoxia treatment (<sup>c</sup> p=0.042). In females we noticed small trend for upregulation although insufficient for reaching level of statistical significance. At the same time, Nrf-2 protein remained unchanged in both sexes.

### 50 The <sup>18</sup>FDG uptake in brain of CBA/H mice

In order to determine if there was any difference between glucose metabolism in brain of CBA/H mice with respect to sex

and/or treatment, we measured brain glucose uptake. The representative pictures of all groups using <sup>18</sup>FDG as a marker are presented in Figure 4 (A – female control, B – male control, C – female hyperoxia, D – male hyperoxia).

Graphical display of glucose consumption in back brain vs. whole brain of CBA/H mice, expressed as a percentage of SUV ratio is presented in Figure 5. The percentage of total SUV in back brain of female control mice was 8% higher in relation to their corresponding male controls (p=0.008). Moreover, glucose consumption in the back brain of hyperoxia-treated females was significantly lower, when compared to normoxia-treated females (p<0.001). In males, we found no difference in <sup>18</sup>FDG uptake in back brain between normoxia and hyperoxia-treated group of animals.

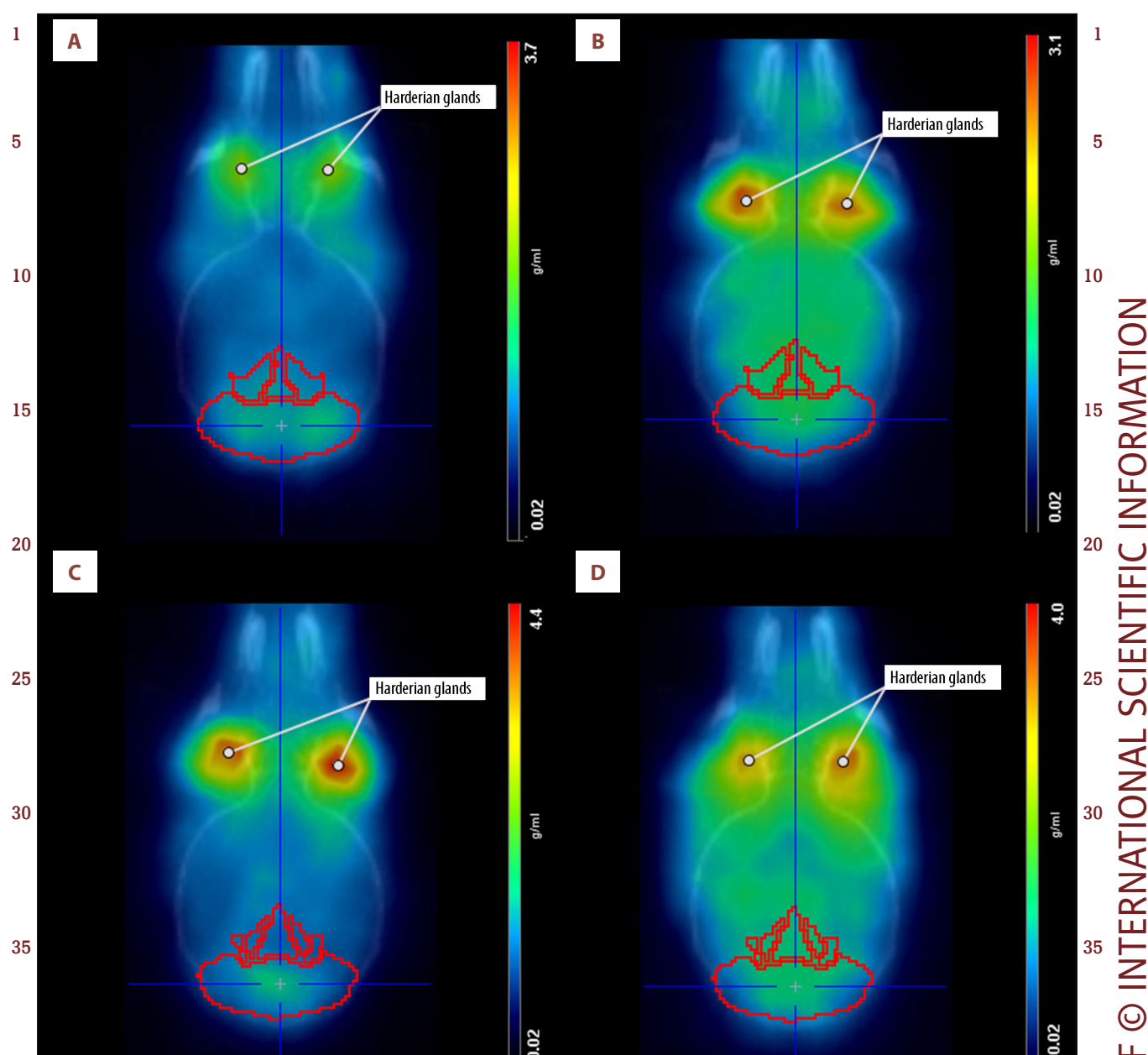


**Figure 4.** Representative PET mouse brain images using  $^{18}\text{F}$ FDG as a marker, visualized and ordered as follows: (A) female control; (B) male control; (C) female hyperoxia; (D) male hyperoxia. The bars represent calculated SUV (g/ml) data of PET mouse brain image co-registered with CT mouse brain template. Region of interest (back brain) is selected. Harderian glands are also annotated. Harderian glands are physiologically highly visible because of their ability to incorporate  $^{18}\text{F}$ FDG from the blood more avidly than any other tissue.

## Discussion

The aim of this study was to investigate sex-related differences in oxidative/antioxidative status in brains of 12-month-old CBA/H mice in response to acute oxidative stress (hyperoxia). We also intended to examine whether hyperoxia had sex-related effect on animals that enter reproductive senescence. It is generally accepted that oxidative damage plays

an important role in neurodegenerative diseases and ageing [1,5,32]. We chose mice aged 12 months as a representative of middle-aged, but still healthy, tumor-free mice [33]. Another reason for choosing 12 months is that mice at the age of 9 to 12 months enter the initial stage of reproductive senescence [34]. Yet another reason for choosing mice in this age range is the more pronounced difference in oxidative/antioxidative status between sexes, as shown in our previous study [33].

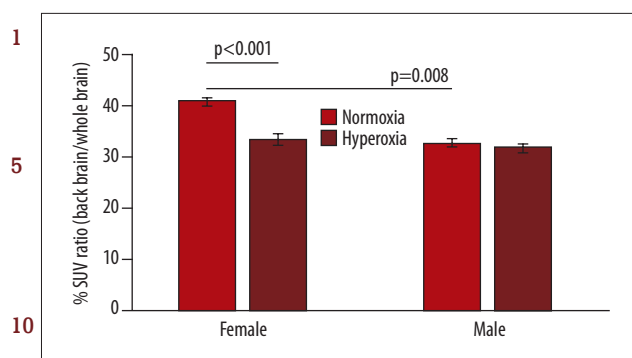


**Figure 5.** Graphical display of glucose consumption in back brain vs. whole brain of CBA/H mice, expressed as a percentage of SUV ratio. Bars represent mean  $\pm$ SD; significant difference in back brain glucose consumption is observed between male and female normoxia-treated mice (\*\* p=0.008), and between female normoxia and hyperoxia-treated mice (\*\*\*) p<0.001), respectively.

hyperoxia [39], when a significant amount of  $H_2O_2$  can diffuse out of mitochondria to cytosol [40]. In our study male mice used increased Cat protein level for hyperoxia protection, while no change in Cat protein was detected in females. Moreover, the increase in both isoforms of Sod without concomitant increase in Cat, leads to accumulation of  $H_2O_2$ . Our data suggest that, among other factors, the lack of Cat activation upon the acute stress load in females may be associated with their increased susceptibility towards the oxidative stress, together with the decline in glucose metabolism in back brain.

Transcriptional factor Nrf-2 is the oxidative stress sensor that activates the expression of stress response genes [41], among which Ho-1 is the best studied [42]. We have found no changes in Nrf-2 upon hyperoxia, regardless of sex. However, the expression of Ho-1 was increased on protein level in hyperoxia-treated males compared to their corresponding normoxic group. Since Ho-1 is a stress response protein and its induction is associated with protection against oxidative stress, females' higher susceptibility could be partially explained by the lack of the upregulation of Ho-1 protein.

Sex difference in the brain glucose metabolism was most profoundly pronounced in the back brain of hyperoxia-treated mice, with females having a lower glucose uptake than males. According to Borrás et al., lower glucose consumption in the brain is correlated with higher  $H_2O_2$  production and oxidative stress [11]. We found no difference between hyperoxia treated and control animals in glucose consumption in the back brain of male mice. However, females in normoxia conditions had higher glucose consumption rate in back brain compared to corresponding male group, which could stand for females' ability to cope better with ROS during normoxia, but impaired capacity to protective response against oxidative stress in hyperoxia conditions. The exact molecular basis of sex-related differences in the brain glucose consumption in conditions of mild oxidative stress is not clearly defined, but is likely to be a complicated interaction involving genomic differences, sex hormones, and metabolites.

## Conclusions

Our results indicate that exposure of 12 months old CBA/H mice to normobaric hyperoxia does not lead to brain oxidative damage, but instead results in redox disturbance as assessed by the antioxidative enzyme alterations, which may be regarded as part of the adaptive response to acute oxidative stress. Data obtained using MicroPET Scan technology with  $^{18}F$ FDG confirmed lower glucose metabolism in the back brain of females upon hyperoxia treatment. This suggests their diminished protection in response to hyperoxia exposure, which might be due to an early stage of menopause, characterized



1 by progressive loss of protection by ovarian hormones in females at that age. We propose this model of hyperoxia as a useful tool to assess sex differences in adaptive response to mild stress conditions, which may be responsible, at least in  
5 part, for observed sex differences in longevity. However, further studies are needed to confirm causal mechanisms responsible for the observed differences.

## 10 References:

1. Muller FL, Lustgarten MS, Jang Y et al: Trends in oxidative aging theories. *Free Radic Biol Med*, 2007; 43: 477–503
2. Beckman KB, Ames BN: The free radical theory of aging matures. *Physiol Rev*, 1998; 78: 547–81
- 15 3. Harman D: Aging: a theory based on free radical and radiation chemistry. *J Gerontol*, 1956; 11: 298–300
4. Sastry J, Pallardo FV, Vina J: The role of mitochondrial oxidative stress in aging. *Free Radic Biol Med*, 2003; 35: 1–8
5. Wright AF, Jacobson SG, Cideciyan AV et al: Lifespan and mitochondrial control of neurodegeneration. *Nat Genet*, 2004; 36: 1153–58
- 20 6. Promislow D<sup>o</sup>: Mate choice, sexual conflict, and evolution of senescence. *Behav Genet*, 2003; 33: 191–201
7. Gruenewald C, Botella JA, Bayersdorfer F et al: Hyperoxia-induced neurodegeneration as a tool to identify neuroprotective genes in *Drosophila melanogaster*. *Free Radic Bio Med*, 2009; 46: 1668–76
8. Landis GN, Abdueva D, Skvortsov D et al: Similar gene expression patterns characterize aging and oxidative stress in *Drosophila melanogaster*. *Proc Natl Acad Sci USA*, 2004; 101: 7663–68
- 25 9. Lewis KN, Mele J, Hayes JD, Buffenstein R: Nrf2, a guardian of healthspan and gatekeeper of species longevity. *Integr Comp Biol*, 2010; 50: 829–43
10. Celik B, Yalcin AD, Bisgin A et al: Level of TNF-related apoptosis-inducing ligand and CXCL8 correlated with 2-[18F]Fluoro-2-deoxy-D-glucose uptake in anti-VEGF treated colon cancers. *Med Sci Monit*, 2013; 19: 875–82
- 30 11. Borras C, Stvolinsky S, Lopez-Gruoso R et al: Low *in vivo* brain glucose consumption and high oxidative stress in accelerated aging. *FEBS Lett*, 2009; 583: 2287–93
12. Sung KK, Jang DP, Lee S et al: Neural responses in rat brain during acute immobilization stress: a [F-18]FDG micro PET imaging study. *Neuroimage*, 2009; 44: 1074–80
- 35 13. Hu H, Su L, Xu YQ et al: Behavioral and [F-18] fluorodeoxyglucose micro positron emission tomography imaging study in a rat chronic mild stress model of depression. *Neuroscience*, 2010; 169: 171–81
14. Lopez-Gruoso R, Gambini J, Abdelaziz KM et al: Early, but not late onset estrogen replacement therapy prevents oxidative stress and metabolic alterations caused by ovariectomy. *Antioxid Redox Signal*, 2014; 20: 236–46
15. Ding F, Yao J, Zhao L et al: Ovariectomy induces a shift in fuel availability and metabolism in the hippocampus of the female transgenic model of familial Alzheimer's. *PLoS One*, 2013; 8: e59825
- 40 16. Šarić A, Sobočanec S, Mačak Šafranko Ž et al: Female headstart in resistance to hyperoxia-induced oxidative stress in mice. *Acta Biochim Pol*, 2014; 61: 801–7
17. Mačak Šafranko Ž, Sobočanec S, Šarić A et al: The effect of 17beta-estradiol on the expression of dipeptidyl peptidase III and heme oxygenase 1 in liver of CBA/H mice. *J Endocrinol Invest*, 2015; 38: 471–79
- 45 18. Leuenberger N, Pradervand S, Wahli W: Sumoylated PPARalpha mediates sex-specific gene repression and protects the liver from estrogen-induced toxicity in mice. *J Clin Invest*, 2009; 119: 3138–48
19. Sobočanec S, Balog T, Kusic B et al: Differential response to lipid peroxidation in male and female mice with age: correlation of antioxidant enzymes matters. *Biogerontology*, 2008; 9: 335–43
- 50 20. Shertzer HG, Clay CD, Genter MB et al: Cyp1a2 protects against reactive oxygen production in mouse liver microsomes. *Free Radic Biol Med*, 2004; 36: 605–17
21. Cox B, Emili A: Tissue subcellular fractionation and protein extraction for use in mass-spectrometry-based proteomics. *Nat Protoc*, 2006; 1: 1872–78

## Acknowledgements

The authors thank Iva Pešun-Medimorec for her excellent technical assistance.

## Conflict of Interest

The authors declare that they have no conflict of interest.

22. Esterbauer H, Schaur RJ, Zollner H: Chemistry and biochemistry of 4-hydroxynonenal, malonaldehyde and related aldehydes. *Free Radic Biol Med*, 1991; 11: 81
23. Paglia DE, Valentine WN: Studies on the quantitative and qualitative characterization of erythrocyte glutathione peroxidase. *J Lab Clin Med*, 1967; 70: 158–69
24. Aebi H: Catalase *in vitro*. *Methods Enzymol*, 1984; 105: 121–26
25. Arthur JR, Boyne R: Superoxide dismutase and glutathione peroxidase activities in neutrophils from selenium deficient and copper deficient cattle. *Life Sci*, 1985; 36: 1569–75
26. Laemmli UK: Cleavage of structural proteins during the assembly of the head of bacteriophage T4. *Nature*, 1970; 227: 680–85
27. Lowry OH, Rosebrough NJ, Farr AL, Randall RJ: Protein measurement with the Folin phenol reagent. *J Biol Chem*, 1951; 193: 265–75
28. Fueger BJ, Czernin J, Hildebrandt I et al: Impact of animal handling on the results of 18F-FDG PET studies in mice. *J Nucl Med*, 2006; 47: 999–1006
29. Ma Y, Hof PR, Grant SC et al: A three-dimensional digital atlas database of the adult C57BL/6J mouse brain by magnetic resonance microscopy. *Neuroscience*, 2005; 135: 1203–15
30. Mirrione MM, Schiffer WK, Fowler JS et al: A novel approach for imaging brain-behavior relationships in mice reveals unexpected metabolic patterns during seizures in the absence of tissue plasminogen activator. *Neuroimage*, 2007; 38: 34–42
31. Pfaffl MW, Horgan GW, Dempfle L: Relative expression software tool (REST) for group-wise comparison and statistical analysis of relative expression results in real-time PCR. *Nucleic Acids Res*, 2002; 30: e36
32. Barja G: Free radicals and aging. *Trends Neurosci*, 2004; 27: 595–600
33. Sverko V, Sobočanec S, Balog T, Marotti T: Age and gender differences in antioxidant enzyme activity: potential relationship to liver carcinogenesis in male mice. *Biogerontology*, 2004; 5: 235–42
34. Diaz Brinton R: Minireview: translational animal models of human menopause: challenges and emerging opportunities. *Endocrinology*, 2012; 153: 3571–78
- 35 35. Ahotupa M, Mantyla E, Peltola V et al: Pro-oxidant effects of normobaric hyperoxia in rat tissues. *Acta Physiol Scand*, 1992; 145: 151–57
36. Clarke DD, Sokoloff L: Circulation and energy metabolism of the brain. In: Siegel GJAB, Albers RW, Fisher SK, Uhler MD (eds.). *Basic Neurochemistry: Molecular, Cellular and Medical Aspects*. 6. ed. Philadelphia: Lippincott-Raven; 1999; 637–70
- 40 37. Ledwozyw A, Borowicz B: The influence of normobaric hyperoxia on anti-oxidant enzymes activities and peroxidation product levels in rat lungs. *Arch Vet Pol*, 1992; 32: 135–41
38. Ho Y-S, Magnenat J-L, Bronson RT et al: Mice deficient in cellular glutathione peroxidase develop normally and show no increased sensitivity to hyperoxia. *J Biol Chem*, 1997; 272: 16644–51
39. Ho YS, Xiong Y, Ma W et al: Mice lacking catalase develop normally but show differential sensitivity to oxidant tissue injury. *J Biol Chem*, 2004; 279: 32804–12
40. Turrens JF, Freeman BA, Crapo JD: Hyperoxia increases H<sub>2</sub>O<sub>2</sub> release by lung mitochondria and microsomes. *Arch Biochem Biophys*, 1982; 217: 411–21
41. Surh YJ, Kundu JK, Na HK: Nrf2 as a master redox switch in turning on the cellular signaling involved in the induction of cytoprotective genes by some chemopreventive phytochemicals. *Planta Med*, 2008; 74: 1526–39
- 50 42. Lee PJ, Alam J, Sylvester SL et al: Regulation of heme oxygenase-1 expression *in vivo* and *in vitro* in hyperoxic lung injury. *Am J Respir Cell Mol Biol*, 1996; 14: 556–68

10

15

20

25

30

35

40

45

50

53